

Synthesis of AuAg/Ag/Au open nanoshells with optimized magnetic plasmon resonance and broken symmetry for enhancing second-harmonic generation†

Tao Zhou,^a Si-Jing Ding,^{*a} Zhi-Yong Wu,^c Da-Jie Yang,^d Li-Na Zhou,^a Zhi-Rui Zhao,^a Liang Ma,^{*b} Wei Wang,^c Song Ma,^c Si-Man Wang,^c Jia-Nan Zou,^c Li Zhou,^c Qu-Quan Wang,^{*c}

^aSchool of Mathematics and Physics, China University of Geosciences (Wuhan), Wuhan 430074, China.

E-mail: dingsijing@cug.edu.cn

^bHubei Key Laboratory of Optical Information and Pattern Recognition, Wuhan Institute of Technology, Wuhan 430205, China.

E-mail: maliang@wit.edu.cn

^cDepartment of Physics, Key Laboratory of Artificial Micro- and Nano-structures of the Ministry of Education, Wuhan University, Wuhan 430072, China.

E-mail: qqwang@whu.edu.cn

^dMathematics and Physics Department, North China Electric Power University, Beijing 102206, China.

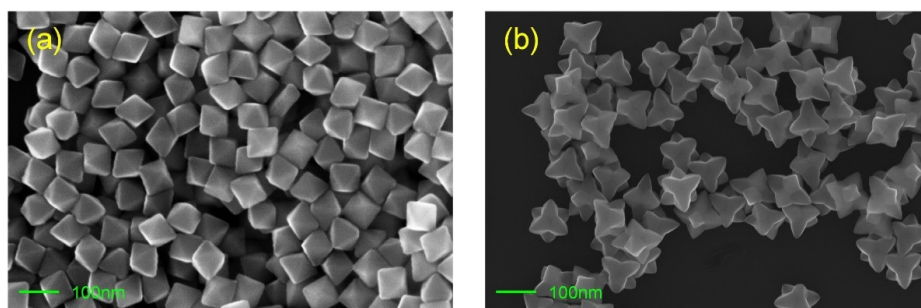


Figure S1. SEM images of PbS templates. (a) PbS nanoctahedron with an average side length of 66.5 ± 2.5 nm. (b) PbS nanostar with an average side length of 316.2 ± 8.8 nm.

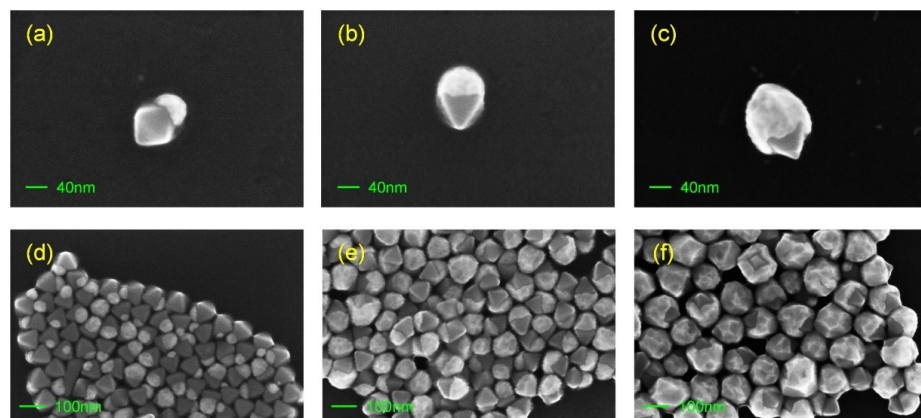


Figure S2. SEM images of Au nanocups grown on PbS nanoctahedron. The corresponding amount of Au (V_{Au1}) is 60 μ L (a, d), 200 μ L (b, e) and 800 μ L (c, f).

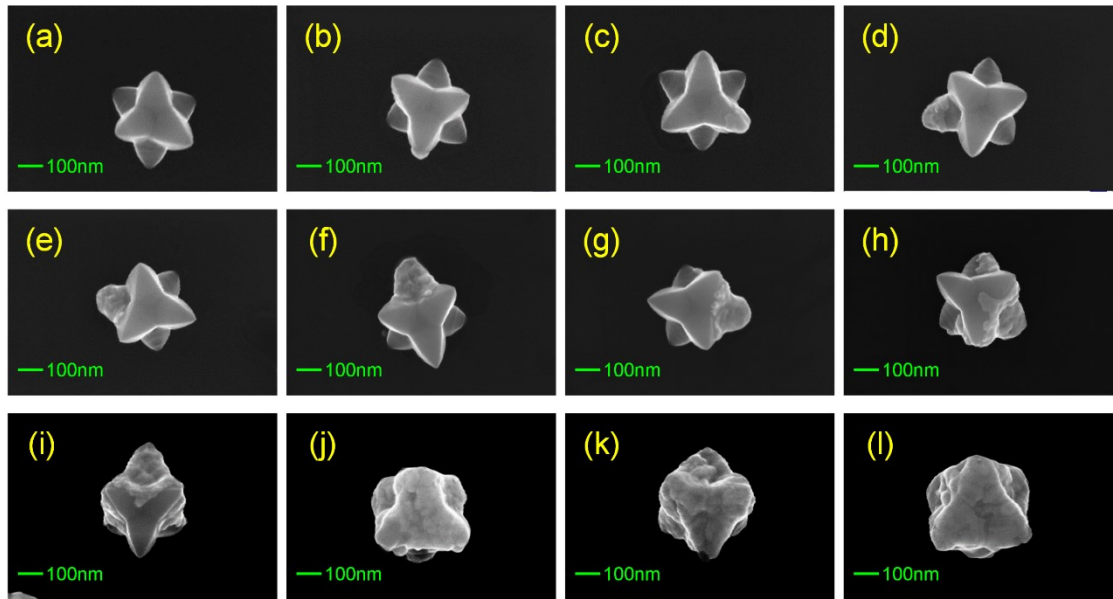


Figure S3. SEM images of Au nanoshell grown on a single PbS nanostar. The corresponding amount of Au (V_{Au1}) is 0 μL (a), 10 μL (b), 40 μL (c), 60 μL (d), 80 μL (e), 100 μL (f), 200 μL (g), 400 μL (h), 500 μL (i), 800 μL (j), 900 μL (k), and 1200 μL (l).

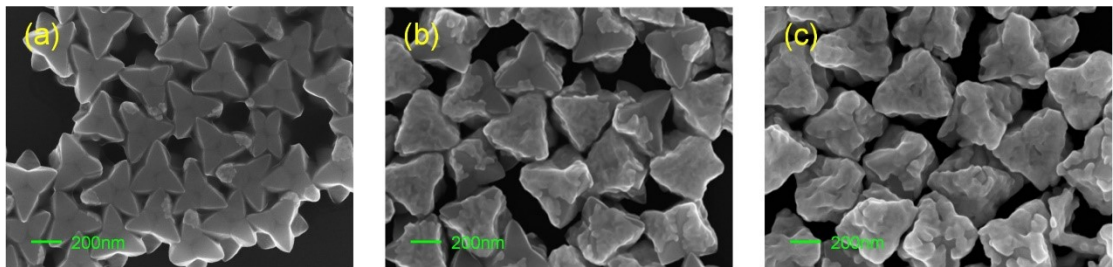


Figure S4. Large-scale SEM images of Au nanoshells grown on PbS nanostars overgrowth with Au open nanoshells. The corresponding amount of Au (V_{Au1}) is 20 μL (a), 500 μL (b) and 900 μL (c).

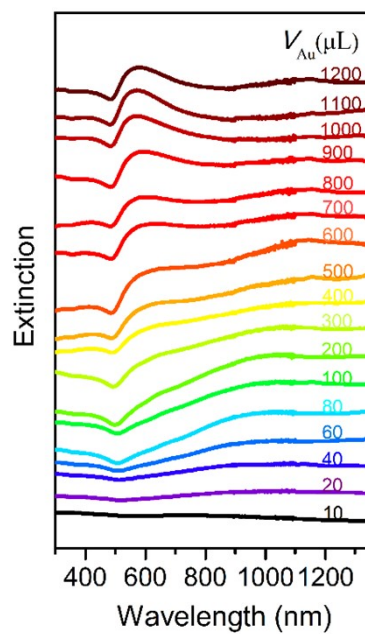


Figure S5. Extinction spectra of Au open nanoshells recorded after dissolving off PbS templates.

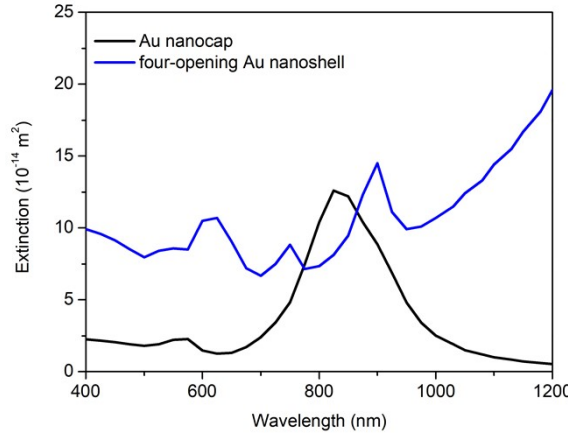


Figure S6. Calculated extinction cross sections of the Au nanocap and four-opening Au nanoshell.

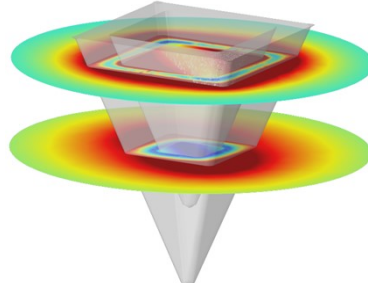


Figure S7. The magnetic field intensity around the nanocap. The magnetic field is mainly at the outer boundary of the nanocap.

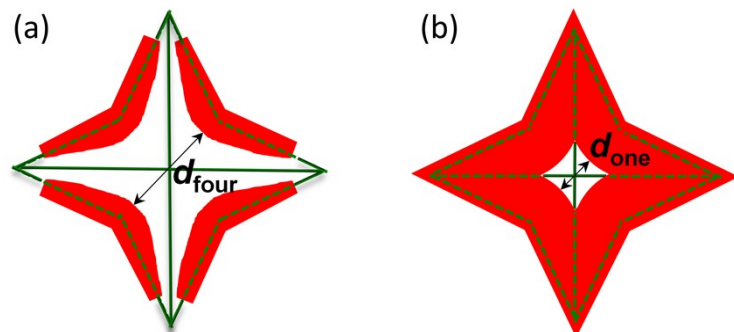


Figure S8. Bottom-view illustrations of the four-opening ($V_{\text{Au1}} = 500 \mu\text{L}$, $d_{\text{four}} = 185.6 \pm 26.8 \text{ nm}$) and one-opening ($V_{\text{Au1}} = 900 \mu\text{L}$, $d_{\text{one}} = 69.3 \pm 12.0 \text{ nm}$) Au nanoshells.

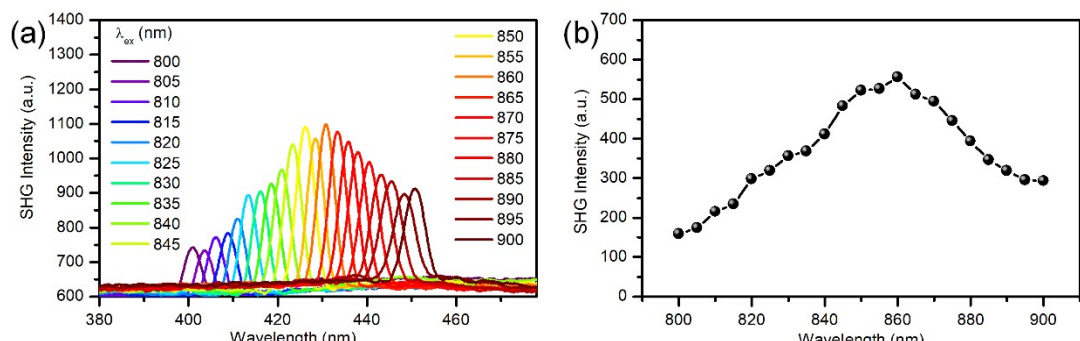


Figure S9. Morphology-dependent SHG of the Au open nanoshells. (a) SHG spectra of the Au open nanoshells ($V_{\text{Au1}} = 1000 \mu\text{L}$) with varied excitation wavelength. (b) SHG excitation spectra with $V_{\text{Au1}} = 1000 \mu\text{L}$.

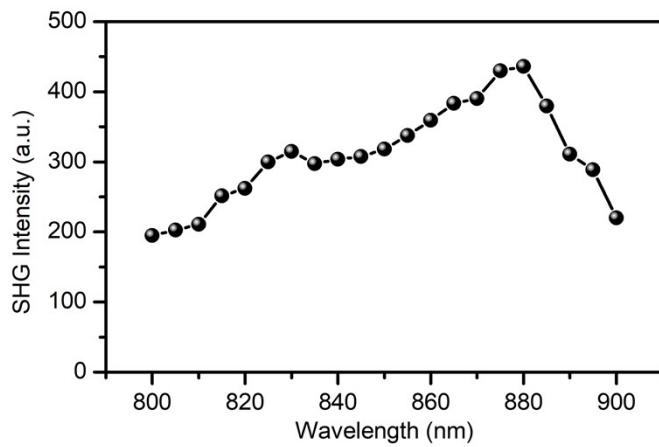


Figure S10. SHG excitation spectra of the Au nanocaps with $V_{\text{Au1}} = 80 \mu\text{L}$. The law of the SHG excitation spectra of the Au nanocaps are similar to those of the four-opening and one-opening Au nanoshells.

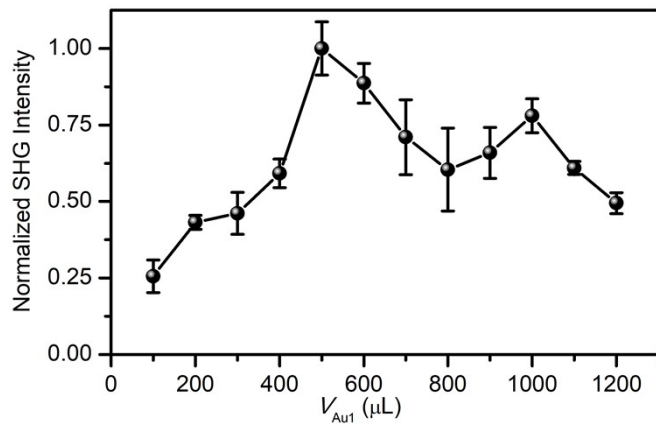


Figure S11. Normalized SHG intensity as a function of V_{Au1} . The excitation wavelength is 880 nm.

Table S1. The Au and Ag atomic content of Au and Ag/Au open nanoshells in the EDX measurement.

Samples	Atomic content	Au (At%)	Ag (At%)
Au open nanoshells		100	0
Ag/Au open nanoshells ($V_{\text{Ag}} = 300 \mu\text{L}$)		78.85	21.15